 CMES, vol.95, no.6, pp.453-482, 2013

A Non-probabilistic Reliability-based Optimization of Structures Using Convex Models

Fangyi Li[1,2], Zhen Luo[3], Jianhua Rong[1] and Lin Hu[1]

Abstract: This paper aims to propose a non-probabilistic reliability-based multi-objective optimization method for structures with uncertain-but-bounded parameters. A combination of the interval and ellipsoid convex models is used to account for the different groups of uncertain parameters, in which the interval model accounts for uncorrelated parameters, while the ellipsoid model is applied to correlated parameters. The design is then formulated as a nested double-loop optimization problem. A multi-objective genetic algorithm is used in the out loop optimization to optimize the design vector for evaluating the objectives, and the Sequential Quadratic Programming (SQP) algorithm is applied in the inner loop to evaluate the uncertain vector and non-probabilistic reliability index. Since the double-loop process for most engineering problems is computationally prohibitive, the polynomial response surface method (RSM) is applied to construct a surrogate model for the approximation of the objective functions and constraints, in order to improve the computational efficiency. In this way, a new reliability-based optimization method is established as a nature combination of the non-probabilistic multi-objective optimization method using convex models with the surrogate model. Typical numerical examples and a practical engineering application are used to demonstrate the effectiveness of the proposed optimization method.

Keywords: Reliability-based optimization, multi-objective optimization, convex models, interval uncertainty, surrogate models.

[1] School of Automotive and Mechanical Engineering, Changsha University of Science and Technology, Changsha, 410114, China.
Corresponding Author: Telephone: +86-731-8525-8630; Fax:+86-731-8525-8630; Email: lfy703@sina.com (Dr.Fangyi. Li)

[2] Key Laboratory of Manufacture and Test Techniques for Automobile Parts, Ministry of Education, Chongqing University of Technology, Chongqing, 400054,China.

[3] School of Mechanical and Mechatronic Systems, University of Technology, Sydney, NSW 2007, Australia

1 Introduction

Multi-objective optimization addresses one of the key problems in the area of engineering optimization [Marler and Arora (2004)]. Most conventional multi-objective optimization methods [Chen, Sahai, Messac, and Sundararaj (2000); Lin, Luo, and Tong (2010); Luo, Chen, Yang, Zhang, and Abdel-Malek (2005)] are under the assumption that the parameters and variables involved are deterministic. However, many real-world problems are too complex to be defined deterministically, because it is impossible to obtain complete information. As a matter of fact, the design optimization of engineering structures involves a variety of uncertainties [Schuëller and Jensen (2008); Valdebenito and Schuëller (2010)], which are inherent in loads, structural parameters, material properties, tolerance, boundary conditions, and geometric dimensions. Hence, the deterministic assumption may lead to unexpected or even unfeasible designs, as in special circumstances the uncertainties may result in significant changes of structural performance [Ben-Haim (1994); Ben-Haim and Elishakoff (1990)]. The optimization of engineering structures under uncertainties offer challenges in many aspects. As a result, uncertainties should be addressed in the process of design optimization, so as to ensure structural safety and avoid breakage and even collapse of structures in extreme working conditions.

Over the past, the design optimization of structures incorporating various uncertainties has experienced considerable development with a range of applications [Olyaie, Razfar, and Kansa (2011); Santos, Matioli, and Beck (2012); Wang, Gao, Yang, and Song (2011)]. Amongst these methods, the reliability-based design optimization (RBDO) provides an effective way to find the best design against the failure of structures subject to uncertainty. For real-world engineering structures, a majority of RBDO problems are in association with multi-objective design requirements. As a result, recently, the reliability-based multi-objective optimization (RBMOO) has much drawn attention for more advanced design problems. Basically, both the probabilistic and non-probabilistic methods can be applied to RBMOO problems in the design of structures.

In the probabilistic methods, uncertain parameters are often treated as random variables with predefined probability distribution functions. For instance, Barakat, Bani-Hani, and Taha (2004) presented a general approach for conducting multi-objective reliability-based design optimization of prestressed concrete beams, using ε-constraint method. Taboada, Baheranwala, Coit, and Wattanapongsakorn (2007) proposed two different schemes, namely the pseudo-ranking and data mining clustering for grouping the data, to reduce the size of the Pareto optimal set in the design of system reliability. Sinha (2007) presented a method for large-scale engineering RBMOO systems, and the uncertainty was quantified using the approximate moment and reliability index methods. Deb, Padmanabhan, Gupta, and Mall (2007)

combined traditional reliability ptimization techniques with evolutionary multiobjective optimization (EMO) for better handling uncertainties of variables and parameters. Khakhal, Nariman-zadeh, Darvizeh, Masoumi, and Notghi (2010) conducted reliability-based robust multiobjective optimization for S-shaped box beams to maximize the energy-absorbing capacity with uncertainties. Fang, Gao, Sun, and Li (2013) proposed multi-objective reliability-based design optimization procedure based on the response surface method and Monte Carlo simulation. From the above studies, it can be found that the probabilistic-based reliability assessment requires sufficient information for constructing precise probability distribution functions. However, it is practically difficult to obtain complete information to determine probability density functions. Furthermore, Ben-Haim and Elishakoff (1990) have shown that even small variations deviating from the real values may cause relatively large errors of the probability distributions in the feasible region. As a result, the probabilistic methods may experience difficulty for complex engineering problems without knowing complete information.

Amongst many methods for non-probabilistic uncertain optimization, the convex models [Ben-Haim (1994); Ben-Haim and Elishakoff (1990); Möller and Beer (2008)] have been widely studied as beneficial supplements to probabilistic methods. The interval and ellipsoid convex models are especially useful for those problems with uncertain-but-bounded parameters, without having to know their precise probability distributions besides the lower and upper bounds. Interval methods are characterized with conceptual simplicity and other merits [Kang and Luo (2009)], in which all possible values of an uncertain parameter are bounded within a one-dimensional convex set, which makes it convenient to measure the uncertainties for the bounded parameters without detailed information. The determination of lower and upper limits for uncertain parameters is much easier than the identification of probability distributions for random variables. As a special case of ellipsoid models, the interval model is more suitable for independent and uncorrelated parameters. However, the overestimation due to the wrapping effect of interval computation will be carefully handled [Wu, Luo, Zhang, Zhang, and Chen (2013); Wu, Zhang, Chen, and Luo (2013)]. Unlike interval models, the ellipsoid model, as a continuously differentiable quantity, more suits correlated parameters with multiple dependencies for a better control of the overestimation.

Ben-Haim (1994) and Elishakoff (1995) may be the first a few researchers, who proposed the concept of non-probabilistic reliability based on convex models. Since then, the RBDO using convex models has been developed and applied to a number of applications [Valdebenito and Schuëller (2010)]. For instance, Elishakoff, Haftka, and Fang (1994) proposed a design approach for structural optimization with uncertain but bounded loads. Lombardi (1998) developed a two-step method

that alternates between optimization and anti-optimization for non-probabilistic optimization of truss structures. Du, Sudjianto, and Huang (2005) studied a RBDO method to deal with the uncertain variables characterized via the mixture of random and interval-valued parameters. Qiu, Yang, and Elishakoff (2008) introduced the interval approach into the RBDO problems, which considered the system failure probability from the statistical parameter intervals. Au, Cheng, Tham, and Zeng (2003) proposed a nested optimization technique for robust-reliability using the convex model, in which the unsatisfactory degrees of the uncertain parameters were used to measure the robust-reliability. Jiang, Han, and Liu (2007) presented an optimization method for structures with uncertain constraints based on a satisfaction degree of interval to accommodate practical problems. Gao (2007) investigated a methodology for the natural frequency and mode shape analysis of truss-type structures involving interval parameters. Lagaros, Garavelas, and Papadrakakis (2008) proposed a seismic optimization method for reliability constrained designs of structures. Luo, Kang, Luo, and Li (2009) studied a non-probabilistic reliability-based topology optimization with ellipsoid models, in which the reliability constraints were re-formulated as equivalent constraints, and it was then extended to such optimization problems with geometrical nonlinearity [Kang and Luo (2009)].

From the literature, it can be found that most existing RBDO optimizations are focused on single objective problems. Relatively, a small number of studies focus on non-probabilistic models and multiple design criteria. However, as mentioned above, a large number of real-world engineering structures are characterized with uncertain-but-bounded parameters and multi-objective design requirements [Ben-Haim and Elishakoff (1990)]. Such design problems are more sophisticated compared to conventional reliability-based optimization problems [Valdebenito and Schuëller (2010)]. More efficient optimization approaches to handle advanced non-probabilistic RBMOO problems are still in demand. Therefore, this paper aims to develop a more efficient method for RBMOO problems by using a combination of interval and ellipsoid convex models.

2 Non-probabilistic reliability index based on convex models

2.1 Convex modeling of uncertainties

As aforementioned, the convex model bounds all possible values of the uncertainties within a convex set without necessarily knowing an inner probabilistic distribution. As aforementioned, the basic convex models typically include the interval model, the ellipsoid model and the multi-ellipsoid model, and etc.

The interval model defines the variation range of the uncertain parameters within an interval, which is bounded by its lower bounded and upper bound. The interval

uncertainty can be expressed as follows:

$$\mathbf{a} \in I^n = \{\mathbf{a} | a_i \in [a_i^L, a_i^R], i = 1, 2, \ldots, n\} \tag{1}$$

The $I^n \subset R^n$ is interval set, which consisting of n parameters. The superscripts L and R denote lower and upper bounds of an interval. In interval models, the nominal (or mean) value and the radius of the interval are expressed as follows:

$$\begin{aligned} \bar{a}_i &= \frac{1}{2}(a_i^L + a_i^R) \\ a_i^w &= \frac{1}{2}(a_i^R - a_i^L) \\ i &= 1, 2, \ldots, n \end{aligned} \tag{2}$$

where $\bar{a}_i$ and a_i^w represent the nominal (or mean) value and radius of an interval, respectively.

The interval model [Gao, Song, and Tin-Loi (2010); Gao, Song, and F. Tin-Loi (2009); Jiang, Han, Liu, and Liu (2008); Li, Luo, and Sun (2011); Li and Azarm (2008)] is known as a hyper-box model for bounded uncertainties, under the assumption that all the uncertain parameters are internally uncorrelated and mutual independently. In practical engineering designs, it is unlikely that all the bounds of uncertain parameters can be reached simultaneously, due to the correlation of the uncertain parameters. In such cases, the interval model may lead to an over-conservative design as a result of the wrapping effect [Wu, Luo, Zhang, Zhang, and Chen (2013)]. For the ellipsoid model [Kang and Luo (2009); Luo, Kang, Luo, and Li (2009)], all the possible values of parameters will be included in a multi-dimensional ellipsoid to represent the uncertainties. It is easy to understand that the interval model is actually a special case of ellipsoid model, and sometimes vice versa. One advantage of the ellipsoid model is that it can incarnate not only the correlations among the uncertain parameters but also the extreme parameter combinations.

In ellipsoid models, unlike the single-ellipsoid model, the multi-ellipsoid model [Kang, Luo, and Li (2011); Luo, Kang, Luo, and Li (2009)] can provide a more flexible and realistic description for the bounded uncertainties. Hence, this study also employs the multi-ellipsoid model to describe some of the uncertain parameters. If $\mathbf{a}$ is assumed as the uncertain vector comprising all uncertain parameters in a multi-dimensional (hyper-) ellipsoid, $\mathbf{a}$ can then be given as follows [Kang, Luo, and Li (2011); Luo, Kang, Luo, and Li (2009)]:

$$\mathbf{a} \in C(\mathbf{W}_\mathbf{a}, \varepsilon) = \{\mathbf{a} : (\mathbf{a} - \bar{\mathbf{a}})^T \mathbf{W}_\mathbf{a} (\mathbf{a} - \bar{\mathbf{a}}) \leq \varepsilon^2\} \tag{3}$$

where $\bar{\mathbf{a}}$ is the nominal value vector of $\mathbf{a}$, $\mathbf{W_a}$ is a real symmetric positive-definite matrix of the convex model, and ε is a real number defining the magnitude of the parameter variability. The vector $\mathbf{a}$ can be change into a dimensionless vector $\boldsymbol{\delta} \in R^n$, and the components of the vector $\boldsymbol{\delta}$ and $\mathbf{a}$ are related by

$$\delta_i = \frac{a_i - \bar{a}_i}{\bar{a}_i} (i = 1, 2, \ldots, n) \tag{4}$$

where $\bar{a}_i$ denotes the nominal value of the i-th uncertain parameter.

Thus, using the dimensionless vector δ_i, the ellipsoid set can be expressed as

$$\boldsymbol{\delta} \in C(\mathbf{W}, \varepsilon) = \{\boldsymbol{\delta} : \boldsymbol{\delta}^T \mathbf{W} \boldsymbol{\delta} \leq \varepsilon^2\} \tag{5}$$

where $\mathbf{W}$ represents the dimensionless characteristic matrix.

In most cases, the uncertainties caused by different parameters can be grouped into different types, such as the independent and uncorrected group, as well as the dependent and corrected group. It is therefore more reasonable to classify entire set of uncertain parameters according to different sources of uncertainties. If we suppose the uncertain variables can be divided into k groups, then we have

$$\mathbf{a}^T = \{\mathbf{a}_1^T, \mathbf{a}_2^T, \ldots, \mathbf{a}_k^T\} \tag{6}$$

With the multi-ellipsoid convex model, each grouped uncertain parameters $\mathbf{a}_i \in R^n (i = 1, 2, \ldots, k)$ can be represented with an individual ellipsoid set as follows:

$$\boldsymbol{\delta}_i \in C_i = \{\boldsymbol{\delta} : \boldsymbol{\delta}_i^T \mathbf{W}_i \boldsymbol{\delta}_i \leq \varepsilon_i^2 (i = 1, 2, \ldots, k)\} \tag{7}$$

where $\boldsymbol{\delta}_i$ is the dimensionless vector of $\mathbf{a}_i$, $\mathbf{W}_i$ denotes the ith characteristic matrix, ε_i is used to define the size of the ith ellipsoid set, k is the number of bounded uncertainties, and n_i is the number of bounded uncertainties in the ith group and $\sum_{i=1}^{k} n_i = n$. It is noted that the sub-vectors included in $\mathbf{a}$ may have different dimensions. In special cases, if each grouped uncertainty consists of only one parameter, $\mathbf{a}$ will degenerate into a multi-dimensional interval set.

The failure status of a structure is represented by the performance function $G(\mathbf{a})$, which indicates failure for a given realization of $\mathbf{a}$ when it is less than or equal to zero. In other words, the performance function is characterized by the limit-state $G(\mathbf{a}) = 0$, which defines a unique surface called the limit state surface. The variable space into a safe region is $G(\mathbf{a}) > 0$ and a failure region is $G(\mathbf{a}) < 0$ by the limit state surface.

2.2 Normalization of the uncertainties

With the convex set for RBO designs, it is more convenient to define an index to quantity the reliability in a normalized parametric space. For this purpose, the following eigenvalue problem is required to be solved via a linear transformation of uncertain parameters [Kang, Luo, and Li (2011); Luo, Kang, Luo, and Li (2009)]:

$$\mathbf{Q}_i^T \mathbf{W}_i \mathbf{Q}_i = \mathbf{\Lambda}_i, \mathbf{Q}_i^T \mathbf{Q}_i = \mathbf{I}(i = 1,2,\ldots,k) \tag{8}$$

In the above equation, $\mathbf{Q}_i$ represents the orthogonal matrix of the normalized eigenvectors, $\mathbf{\Lambda}_i$ is used to denote the diagonal matrix of the eigenvalues of $\mathbf{W}_i$, and $\mathbf{I}$ is an identity matrix. If we define the following vector

$$\mathbf{u}_i = \left(\frac{1}{\varepsilon_i}\right) \mathbf{\Lambda}_i^{1/2} \mathbf{Q}_i^T \boldsymbol{\delta}_i, (i = 1,2,\ldots,k) \tag{9}$$

Then the original convex model in Equation (7) becomes

$$C = \{\mathbf{u} : \mathbf{u}_i^T \mathbf{u}_i \leq 1(i = 1,2,\ldots,k)\} \tag{10}$$

Here $\mathbf{u}_i$ is used to indicate the normalized vector of the i-th grouped uncertain variables $\mathbf{a}_i$. In doing so, the ellipsoids are transformed into spheres of unit radius in the normalized $\mathbf{u}$ space.

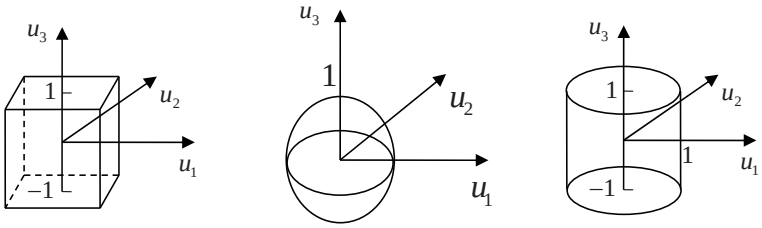

Figure 1: Convex models (e.g. 3 uncertain parameters): (a) 3D interval model; (b) 3D single-ellipsoid model; (c) Muti-ellipsoid model involving an ellipsoid (u_i and u_2) and an interval (u_3)

For the case of a hyper box model, the standard form in (10) degenerates to

$$C = \{\mathbf{u} : \mathbf{u}_i^2 \leq 1(i = 1,2,\ldots,k)\} \tag{11}$$

where the normalized variables $\mathbf{u}_i = (a_i - \bar{a}_i)/a_i^w$. The interval model and the ellipsoid model can be treated as the specific case of the multi-ellipsoid, so this paper focuses on the multi-ellipsoid model, which is schematically shown as Fig.1a-c.

Following the above transformation, the performance function $G(\mathbf{a})$ in the original space changes to the function $g(\mathbf{u})$. The normalized space ($\mathbf{u}$-space) is thus divided into two different regions, namely a safe region ($g(\mathbf{u}) > 0$) and a failure region ($g(\mathbf{u}) < 0$).

2.3 Definition of the non-probability reliability index

2.3.1 Interval model

Here only a simple case with two uncertain parameters is considered to show a quantified measure, in which each uncertain parameter is modeled with an interval set, respectively. Since the structural variations can be measured by the side-length of the corresponding box in the u-space, it can be seen from Fig. 2 that the convex set is denoted by $\{\mathbf{u} = \{u_1, u_2\} : |u_i| \leq 1, |u_2| \leq 1\}$. Here, the infinity norm (or maximum norm) $||\mathbf{u}||_\infty = \max(|u_1|, |u_2|)$ is defined as the length of a vector $\mathbf{u}$ in the u-space. In terms of the infinity norm, the bounds of uncertainties can be defined as $||q||_\infty = 1$. Based on the normalization, the reliability index can then be described as follows [Kang, Luo, and Li (2011); Luo, Kang, Luo, and Li (2009)]:

$$\eta = \text{sgn}(g(\mathbf{0}) \cdot \min(\max|u_1|, |u_2|, \ldots, |u_k|), \text{s.t.} g(\mathbf{u}) = 0 \tag{12}$$

where $\text{sgn}(\cdot)$ is the function that is applied to define a negative reliability index, when the limit-state function is negative at the origin in the $\mathbf{u}$-space [Luo, Kang, Luo, and Li (2009)], which is given as

$$\text{sgn}(x) = \begin{cases} 1 & \text{if } x > 0 \\ 0 & \text{if } x = 0 \\ -1 & \text{if } x < 0 \end{cases} \tag{13}$$

2.3.2 Single ellipsoid convex model

As given in Fig 3, this section is considering the case that the uncertainties are modeled via a single-ellipsoid with two uncertain parameters in a 2D $\mathbf{u}$-space. This figure shows that the maximum allowable variability of the uncertainties is actually determined by the distance from the origin point to the limit-state curve in the $\mathbf{u}$-space. The Euclidean norm is used to measure the length. Thus, the reliability index for a structure design with the single-ellipsoid model can be express as

$$\eta = \text{sgn}(g(\mathbf{0})) \cdot \min(\sqrt{\mathbf{u}^T \mathbf{u}}), \text{s.t. } g(\mathbf{u}) = 0 \tag{14}$$

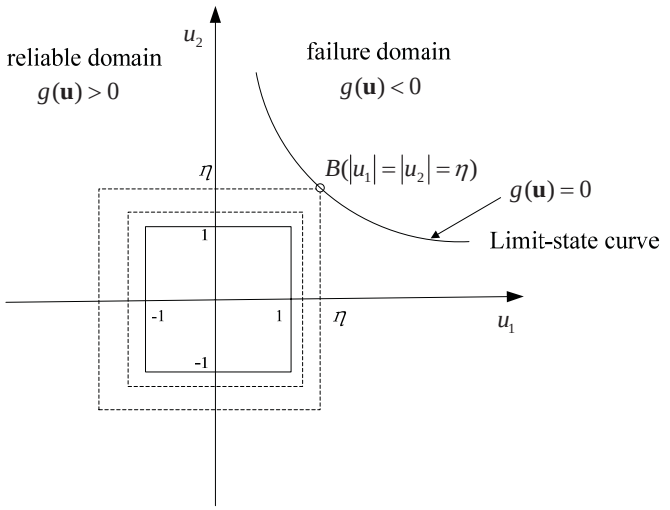

Figure 2: Non-probabilistic reliability index in case of two interval variables for uncertainty description

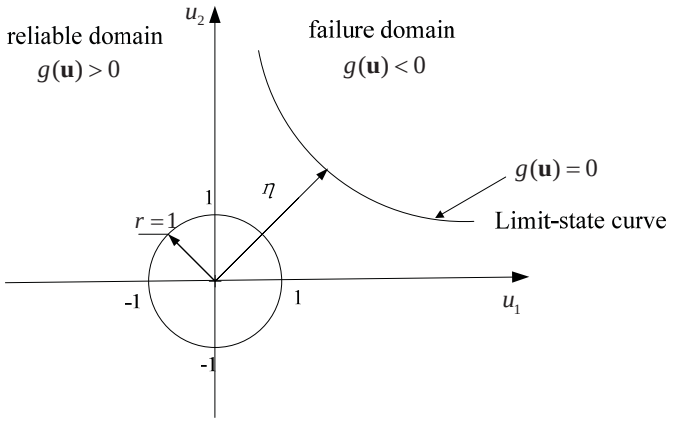

Figure 3: Non-probability reliability index for a case of a single two dimensional ellipsoid

2.3.3 Extension to multi-ellipsoid convex model

In practical designs, in some cases, the uncertainties generated from different sources (e.g. the geometry, material property and external loads) may form different groups, which will be characterized with correlation inside each group but exhibit independence among different groups. Therefore, it is required to consider the grouped

uncertainties for more general and complicated engineering designs under various uncertainties.

Fig. 4 shows the three dimensional u-space of multi-ellipsoid model. For the multi-ellipsoid model to measure the k groups of uncertainties, the infinity norm of the vector consisting of the Euclidean norms of the k standard uncertainty vector [Kang, Luo, and Li (2011); Luo, Kang, Luo, and Li (2009)] can be defined in the $\mathbf{u}$-space as

$$||\mathbf{u}|| = ||\sqrt{\mathbf{u}_1^T\mathbf{u}_1}, \sqrt{\mathbf{u}_2^T\mathbf{u}_2}, \ldots, \sqrt{\mathbf{u}_k^T\mathbf{u}_k}||_\infty = \max(\sqrt{\mathbf{u}_1^T\mathbf{u}_1}, \sqrt{\mathbf{u}_2^T\mathbf{u}_2}, \ldots, \sqrt{\mathbf{u}_k^T\mathbf{u}_k}) \tag{15}$$

The bounds of the normalized multi-ellipsoid convex set can thus be expressed as $||\mathbf{u}|| = 1$. From Fig. 4,the green point has the minimal distance in the sense of the length measure defined in Eq. (15).

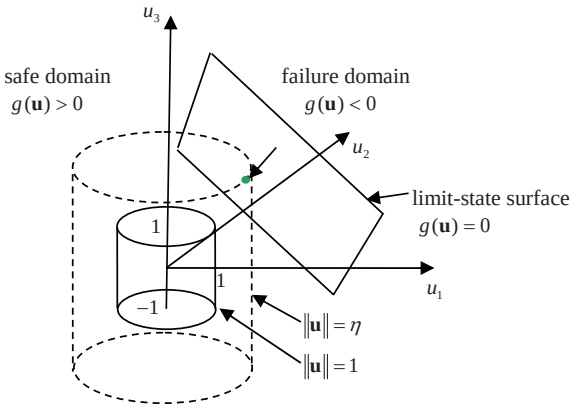

Figure 4: Non-probability reliability index for a case of a multi-ellipsoid model

It is more reasonable to define the non-probabilistic reliability index η as follows [Kang, Luo, and Li (2011); Kang and Luo (2009)]:

$$\eta = \text{sgn}(g(\mathbf{0})) \cdot \min\left(\max\left(\sqrt{\mathbf{u}_1^T\mathbf{u}_1}, \sqrt{\mathbf{u}_2^T\mathbf{u}_2}, \ldots, \sqrt{\mathbf{u}_k^T\mathbf{u}_k}\right)\right) \tag{16}$$

Here, Eq. (16) represents a min-max problem, which will make the evaluation of the reliability index inefficient. According to the research [Kang and Luo (2009); Kang, Luo, and Li (2011)], the above problem can be transformed into the follow-

ing optimization by introducing an augmented variable λ

$$\begin{cases} \eta = \operatorname{sgn}(g(\mathbf{0})) \cdot \min\limits_{\mathbf{u},\lambda} \lambda \\ \text{s.t. } g(\mathbf{u}) = 0 \\ \sqrt{\mathbf{u}_i^T \mathbf{u}_i} - \lambda \leq 0, i = 1, \ldots, k \end{cases} \tag{17}$$

Obviously, a larger η implies that the design allows for a larger parameter variation. For $\eta = 1$, the limit-state surface intersects the boundary of the convex model used for modeling the reference variability of the uncertainty, which indicates that the structure is critical for the reference parameter uncertainties. If $\eta > 1$, the actual fluctuations of structural performance cannot reach failure surface, which means that the structure is reliable.

3 Non-probabilistic reliability-based multi-objective optimization

3.1 Formulation of optimization problem

Generally, the non-probabilistic reliability-based multi-objective optimization (NRMO) problem can be defined in the following form:

$$\begin{aligned} &\min_x \{f_1(\mathbf{x}, \mathbf{a}), f_2(\mathbf{x}, \mathbf{a}), \ldots, f_m(\mathbf{x}, \mathbf{a})\} \\ &\text{s.t. } \eta_j[g_j(\mathbf{x}, \mathbf{u}) \geq 0] \geq \eta_{tj}, j = 1, 2, \ldots, p \\ &\mathbf{x}_l \leq \mathbf{x} \leq \mathbf{x}_r \end{aligned} \tag{18}$$

where

$$\begin{cases} \eta_j = \operatorname{sgn}(g_j(\mathbf{0})) \cdot \min\limits_{\mathbf{u},\lambda} \lambda \\ \text{s.t. } g(\mathbf{u}) = 0 \\ \sqrt{\mathbf{u}_i^T \mathbf{u}_i} - \lambda \leq 0, i = 1, \ldots, k \end{cases}$$

where $f_i(\mathbf{x}, \mathbf{a})(i = 1, 2, \ldots, m)$ is the objective function to be minimized. $\mathbf{x}$ is a design vector, and $\mathbf{x}_l$ and $\mathbf{x}_r$ denote the upper and lower bounds of $\mathbf{x}$, respectively. It should be noted that the design vector $\mathbf{x}$ can also be the mean nominal value of geometrical dimensions and material properties, when their variation are modeled as bounded uncertainties. $\mathbf{a}$ is an uncertain vector described by bounded uncertainties. $\mathbf{u}$ is the normalized vector of uncertain vector $\mathbf{a}$. $g_j(\mathbf{x}, \mathbf{u})$ is the jth structural behavior function. $\eta_j[g_j(\mathbf{x}, \mathbf{u}) \geq 0]$ is the reliability index associated with the performance constraint $g_j(\mathbf{x}, \mathbf{u}) \geq 0$ and η_{tj} is the corresponding specified target reliability index and p is the number of constraints.

In the aforementioned design problem, the evaluation of the reliability index for the jth limit-state function is a 'min-max' type optimization. The problem in (18) is therefore a nested double-loop optimization, in which the outer loop is to minimize the objective functions, while the inner loop is for reliability analysis.

3.2 Implementation of the approximation optimization

To avoiding the expensive computational cost, the surrogate model (or metamodel) [Chau, Han, Bai, and Jiang (2012); Li, Luo, and Sun (2011); Myers and Montgomery (1995); Simpson, Poplinski, Koch, and Allen (2001)], rather than the actual simulation model, will be applied to evaluate the uncertain functions. Eq. (18) can be further formulated as:

$$\min_{\mathbf{x}}\{\tilde{f}_1(\mathbf{x},\mathbf{a}),\tilde{f}_2(\mathbf{x},\mathbf{a}),\ldots,\tilde{f}_m(\mathbf{x},\mathbf{a})\},\text{s.t. } \eta_j[\tilde{g}_j(\mathbf{x},\mathbf{u})\geq 0]\geq \eta_{tj}, j=1,2,\ldots,p, \quad (19)$$

where $\tilde{f}_i(i=1,2,\ldots,m)$ and $\tilde{g}_j(j=1,2,\ldots,p)$ are the surrogate models of the original objectives and constraints, respectively.

In this study, the polynomial response surface method (RSM) technique [Draper and Smith (1998); Myers and Montgomery (1995)] is adopted to construct the surrogate model for the objective functions $\tilde{f}(\mathbf{x},\mathbf{a})$ and constraints $\tilde{g}(\mathbf{x},\mathbf{a})$ in the design space and uncertainty space, respectively. The RSM is a statistical and mathematical method that gives an effective practical means for design optimization. The behavior of RSM is expressed by the approximation as a polynomial on the basis of observation data. That is, the RSM is developed to represent the relationship between the input and output of a physical experiment by a simple mathematical expression, based on the statistical techniques of regression analysis and the analysis of variance to create the approximation models.

The surrogate modeling technique involves two important steps: namely, sampling and constructing approximation model. So, in the aforementioned RSM approach, one of the important steps for successfully constructing the surrogate model is to obtain proper sample points from the design and uncertainty spaces. Usually, the design of experiment (DOE) can be used for this purpose. In this paper, the Latin Hypercube Design (LHD) [Morris and Mitchell (1995)] is employed to generate the sampling points. LHD in general can ensure a well-representative distribution of points over the design and uncertain spaces of variables. In this paper, the LHD algorithm in the ISight software is used to create LHD design matrix for training all sets of sample points. After obtaining the sampling points, the surrogate model can be constructed based on the data.

The solution process of the approximation optimization problem is shown in Fig. 5. In current design domain and uncertain space, $\mathbf{x}$ and $\mathbf{a}$ are both used as the input

variables, and one set of sample points can be obtained by the LHD technique. The surrogate models of objective functions and constraints can be subsequently constructed. After that, the optimization can be performed based on these surrogate models. In Fig. 5, the optimization comprises a double-loop procedure. In this paper, through the Matlab Optimization Toolbox^{TM}, the outer layer optimization is solved by the Non-dominated Sorting Genetic Algorithm II (NSGA-II) developed by [Deb (2001); Deb, Pratap, Agarwal, and Meyarivan (2002)], and the inner layer optimization is solved by Sequential Quadratic Programming (SQP) [Boggs and Tolle (1995)].

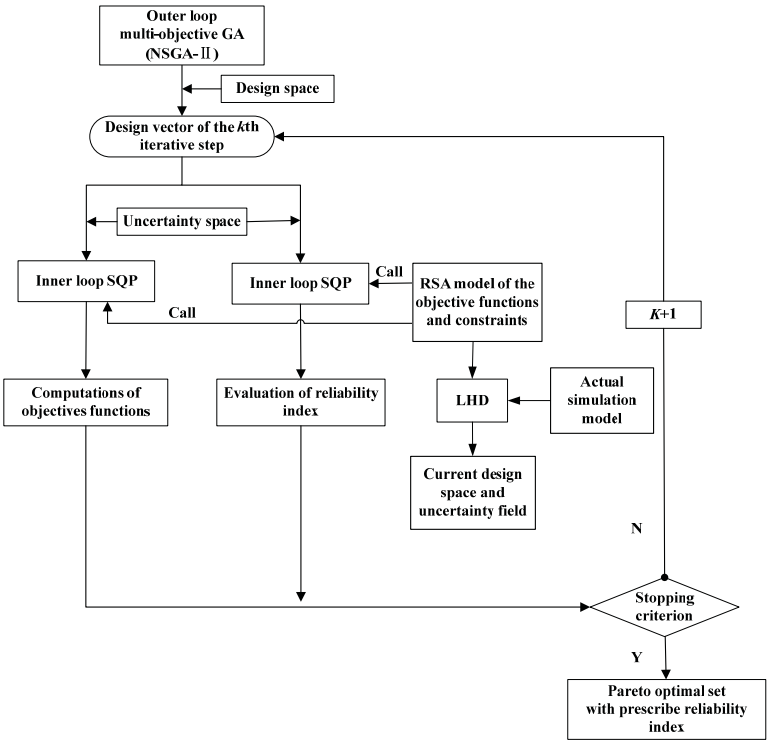

Figure 5: Flow chart for non-probabilistic RBMOO problems

In the outer layer, the NSGA-II [Deb (2001); Deb, Pratap, Agarwal, and Meyarivan (2002)] is first used to generate an amount of individuals, and each individual chromosome denotes a candidate decision vector $\mathbf{x}$. NSGA-II is a computationally fast elitist multi-objective algorithm based on a non-dominated sorting scheme, including the non-dominated sorting for fitness assignments, the fast non-dominated sorting technique, and a crowding distance to rank and select the population fronts.

Then, the algorithm applies the crossover and mutation operators to combine the current population with its offspring generated as next generation. Finally, the best individuals in terms of non-dominance and diversity are selected as the solutions.

In the inner layer optimization, the SQP [Boggs and Tolle (1995)] is used as optimization operator. For each $\mathbf{x}$, the non-probabilistic reliability index for each individual is evaluated based on Eq. (17). The SQP is a nonlinear programming method which starts from a single searching point and finds a solution with the gradient information. It outperforms every nonlinear programming method in terms of efficiency, accuracy, and percentage of successful solutions, over a large number of test problems. The outer NSGA-II will call the SQP in the inner layer to approximate the objective functions and constraints, based on the RSM model for each individual. SQP is applied to evaluate the non-probabilistic reliability index for each individual. Finally, the Pareto set can be obtained with the prescribed reliability index based on Eq. (19).

4 Numerical examples

4.1 Numerical test example

The following numerical example is analyzed firstly as a benchmark example to test the effectiveness of the proposed uncertain optimization methodology. The optimization problem is defined as

$$\begin{aligned}
&\min_{\mathbf{x}} f_1(\mathbf{x},\mathbf{a}) = a_1(x_1+x_2-7.5)^2 + a_2^2(x_2-x_1+3)^2/4 \\
&\quad f_2(\mathbf{x},\mathbf{a}) = a_1^2(x_1-1)^2/4 + a_2^3(x_2-4)^2/2 \\
&\quad \text{s.t. } \eta_j[g_j(\mathbf{x},\mathbf{a}) \geq 0] \geq \eta_{tj}, j = 1,2, \\
&\quad 0 \leq x_1 \neq 5, 0 \leq x_2 \leq 3
\end{aligned} \tag{20}$$

where the performance constraints, g_j, $j = 1,2$, are defined as follows:

$$\begin{aligned}
g_1(\mathbf{x},\mathbf{a}) &= 2.5 - a_1^2(x_1-2)^3/2 - a_2 x_2 \\
g_2(\mathbf{x},\mathbf{a}) &= -a_1^3 x_2 - a_2^2 x_1 + 3.85 + 8a_2^2(x_2-x_1+0.65)^2
\end{aligned} \tag{20a}$$

where the design variables $\mathbf{x} = \{x_1, x_2\}^T$ are regarded as interval parameters with a 3% variation about their nominal values to indicate the level of the uncertainty. The uncertain parameter vector $\mathbf{a} = \{a_1, a_2\}^T$ are bounded by $C = \{\boldsymbol{\delta} : \boldsymbol{\delta}^T \mathbf{W} \boldsymbol{\delta} \leq 0.1^2\}$, where their nominal values are $\bar{\mathbf{a}} = \{\bar{a}_1, \bar{a}_2\}^T = \{1.0, 1.0\}^T$ and the characteristic matrix is $W_a = [1\ 0; 0\ 4]$. The parameters for NSGA-ï¿½ï¿½ algorithm are given in Table 1.

Table 1: NSGA-II parameters

GA parameter name	Value
Population size	50
Number of generation	200
Probability of crossover	0.9
Distribution index for crossover	20
Distribution index for mutation	20

Table 2: Summary of results for the numerical example 1

Pareto points	$\eta_1 = \eta_2 = 1.0$		$\eta_1 = \eta_2 = 1.5$	
Design vector x	(2.9532, 1.7321)	(0.8016, 3.000)	(2.9196, 1.6217)	(0.7067,3.000)
Minimum f_1	8.7137		9.4784	
Minimum f_2		0.5098		0.5215
Reliability index η_1 *(constraint 1)*	1.0080	1.0	1.5012	1.5001
Reliability index η_2 *(constraint 2)*	1.0490	10.7148	1.5253	11.1987
Pareto points	$\eta_1 = \eta_2 = 2.0$		*Deterministic Results*	
Design vector x	(2.8839, 1.5127)	(0.6118, 3.000)	(3.0117, 1.9817)	(0.9999, 3.000)
Minimum f_1	10.2943		7.2534	
Minimum f_2		0.5377		0.5
Reliability index η_1 *(constraint 1)*	2.0092	2.0003	0.0017	0.00056
Reliability index η_2 *(constraint 2)*	2.0160	11.6794	0.0079	9.6991

The optimal result under different reliability indices 1.0, 1.5 and 2.0 is listed in Table 2. It can be found that the minimum f_1 and minimum f_2 increase with increase in the reliability index. This is because that a larger reliability index will generate a smaller feasible zone of the constraints, which leads to a worse value of the objective function. The nominal value-based deterministic optimization result, which is unreliable in presence of uncertainties, is also listed in the Table. It can be seen from the result that the NRMO presents more reliable designs than the deterministic approach.

Fig. 6 plots the Pareto optimal fronts for different reliability indices. The ranges and shapes of the Pareto optimal font vary with the different target reliability indices. When different reliability-based optimizations are conducted, the Pareto front shifts, which depends on the target reliability indices prescribed. It can be seen that the deterministic optimization results are given in the Fig. 6.

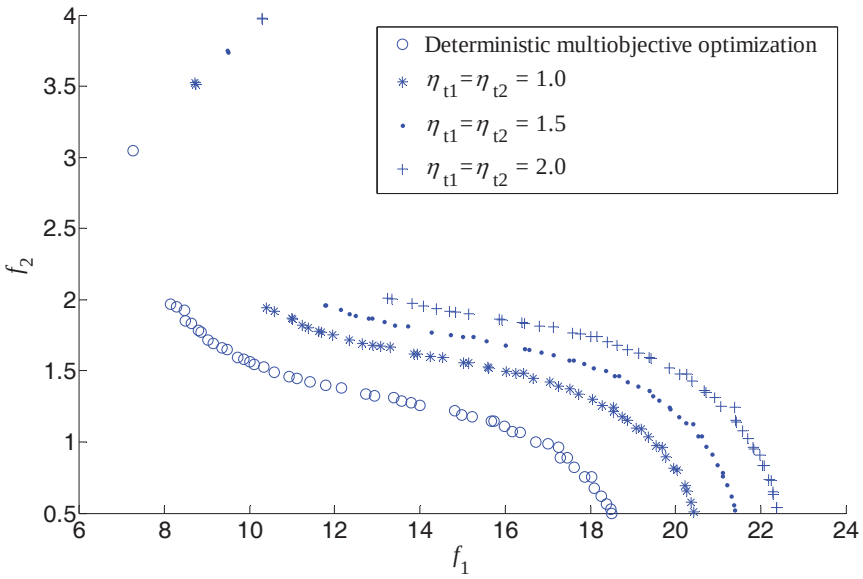

Figure 6: Comparison of Pareto optimal fronts in the deterministic optimization, and the proposed reliability-based optimizations with different reliability index

4.2 Example of cantilever beam

The second example is a structural optimization problem of cantilever beam [Jiang, Han, and Liu (2007); Jiang, Han, Liu, and Liu (2008)] as shown in Fig. 7. This problem aims to minimize both the vertical deflection f_1 of an I-beam sectional structure for a given loads and the cross-sectional area f_2, while satisfying the stress constraint. The design vector is $\mathbf{x} = [x_1, x_2, x_3, x_4]^T$, in which x_1 and x_2 are bounded by an ellipsoid (C^1) and the x_3 and x_4 are bounded by another ellipsoid (C^2)

$$C^1 = \left\{ \delta_{x_1}, \delta_{x_2} : \{\delta_{x_1}, \delta_{x_2}\} \begin{bmatrix} 1 & 0 \\ 0 & 1 \end{bmatrix} \begin{Bmatrix} \delta_{x_1} \\ \delta_{x_2} \end{Bmatrix} \leq 0.05^2 \right\} \tag{21a}$$

$$C^2 = \left\{ \delta_{x_1}, \delta_{x_2} : \{\delta_{x_3}, \delta_{x_4}\} \begin{bmatrix} 1 & 0 \\ 0 & 1 \end{bmatrix} \begin{Bmatrix} \delta_{x_3} \\ \delta_{x_4} \end{Bmatrix} \leq 0.02^2 \right\} \tag{21b}$$

where their nominal values are $\bar{\mathbf{x}} = \{\bar{x}_1, \bar{x}_2, \bar{x}_3, \bar{x}_4\}^T$. The given parameters include Young's Modulus of Elasticity $E = 2.1 \times 10^4 kN/cm^2$, highest transverse forces $P = 600kN$, $Q = 50kN$ and $L = 200cm$.

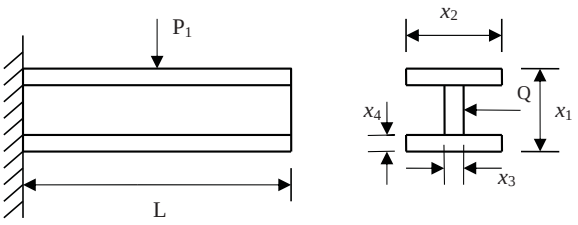

Figure 7: Design problem of cantilever beam

The NRMO problem can be written as below:

$$\min_{x}: \begin{cases} f_1(\mathbf{x}) = \frac{F_1 L^3}{48EI_z} = 500 \Big/ \left(\frac{1}{12} x_3 (x_1 - 2x_4)^3 + \frac{1}{6} x_2 x_4^3 + 2x_2 x_4 \left(\frac{x_1 - x_4}{2} \right)^2 \right) \\ f_2(\mathbf{x}) = 2x_2 x_4 + x_3 (x_1 - 2x_4) \end{cases} \tag{21c}$$

s.t. $\eta_j [g_j(\mathbf{x}) \leq 6kN/cm^2] \geq \eta_{tj}, j = 1$

where $10.0cm \leq x_1 \leq 80.0cm$, $10.0cm \leq x_2 \leq 50.0cm$, $0.9cm \leq x_3 \leq 5cm$ and $0.9cm \leq x_4 \leq 5cm$ are the lateral constraints of design variables, respectively. The constraint $g_j(j = 1)$ is defined as

$$g_1(\mathbf{x}) = \frac{180000x_1}{x_3(x_1 - 2x_4)^3 + 2x_2x_4[4x_4^2 + 3x_1(x_1 - 2x_4)]} + \frac{15000x_2}{(x_1 - 2x_4)x_3^3 + 2x_4x_2^3} \tag{21d}$$

Similarly, the specific parameters for NSGA-II can refer to that given in Table 1.

The Pareto sets with several different target reliability indices are plotted in Fig. 8, respectively. It can be found that the '*span*' of the reliability-based Pareto optimal fronts with a larger reliability index is smaller than that of a smaller reliability index in this example. It can also be found that the '*span*' of NRMO Pareto set is larger than the deterministic optimization. The results with the different reliability index $\eta_{t1} = 1.0$, $\eta_{t1} = 3.0$, $\eta_{t1} = 4.0$ as summarized in Table 3, which show that the minimum objective f_2 increases when the reliability index increases. This is understandable because the increase of the target reliability will often lead to a safer design, but f_1 does not show such a definitive pattern. This might be the reason that the constraint dominates the optimization process of this objective function, as reported in the work of [Sinha (2007)]. From the Table 3, the deterministic optimal design results in a violation of the reliability constraint.

4.3 Thin-wall column crashworthiness design

Thin-walled structure often plays a key role in absorbing crushing energy of a vehicle while frontal and rear collisions occur [Liao, Li, Yang, Zhang, and Li (2008)].

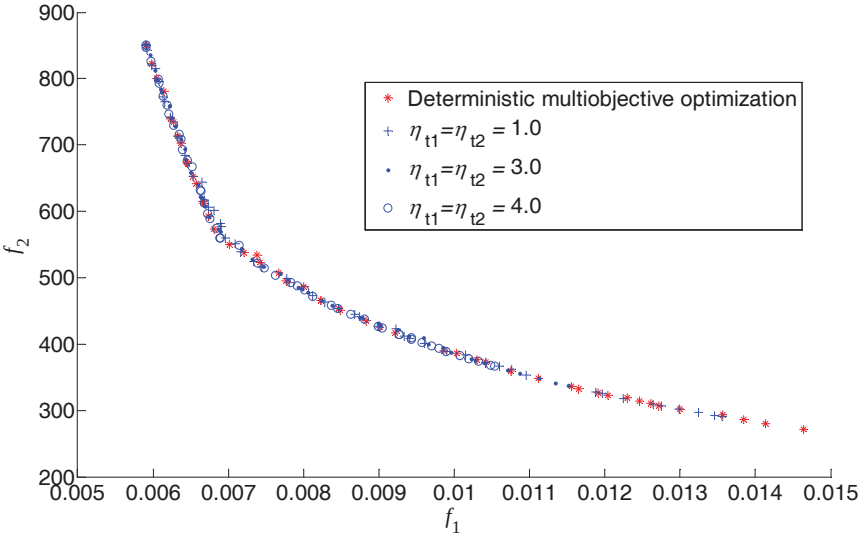

Figure 8: Pareto optimal front for different reliability index

Table 3: Summary of results for the cantilever beam example

Pareto points	$\eta_{t1}=1.0$		$\eta_{t1}=3.0$	
x	(80, 50, 5.0, 5.0)	(80, 50, 0.90,2.23)	(80, 50, 5.0, 5.0)	(80,50, 0.9,2.7)
Min: f_1	5.90×10^{-3}		5.90×10^{-3}	
Min: f_2		290.47		336.87
η_1	8.5247	1.0018	8.5247	3.001
Pareto points	$\eta_{t1}=4.0$		*Deterministic*	
x	(80, 50, 5.0, 5.0)	(80, 49.45, 0.90, 3.03)	(80, 50, 5.0 5.0)	(79.99, 49.72, 0.90, 2.0)
Min: f_1	5.90×10^{-3}		5.90×10^{-3}	
Min: f_2		366.33		271.4293
η_1	8.5247	4.001	8.5247	0.0015

It is thus important to optimize these thin-walled structures for required crashworthiness multi-criteria [e.g. Li, Luo, Rong, and Zhang (2013); Sun, Li, Hou, Zhou, Li, and Li (2010); Xiang, Wang, Fan, and Fang (2006)]. This example is concerned with a thin-walled column in the design context of the proposed reliability-based multi-objective optimization.

The thin-walled column is considered to impact onto a rigid wall with the initial velocity of $13.8m/s$ and $40ms$ time duration (Fig. 9). As denoted in the research [Li, Luo, Rong, and Zhang (2013); Sun, Li, Hou, Zhou, Li, and Li (2010); Xiang,

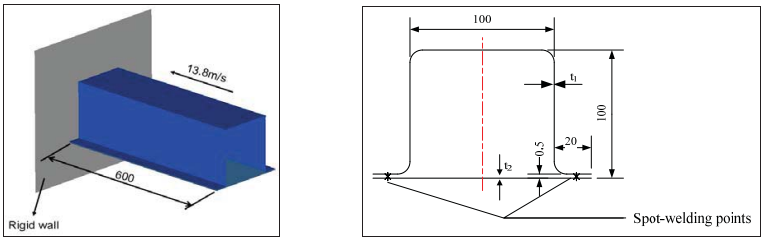

Figure 9: A thin-walled column impacting into the rigid wall and design variable and geometric parameters

Wang, Fan, and Fang (2006)], typically the concerned responses in crashworthiness designs are deformations, velocities, accelerations, intrusions, section forces, rigid wall forces, absorbed energy and etc.

In this study, the maximum internal energy E_d and the mass/weight W of the thin-walled column are used as the objective functions. The average rigid wall force g_m is treated as a constraint. The thicknesses t_1 and t_2 are chosen as the design variables. It is assumed that the material properties, geometrical dimensions are uncertain-but-bounded parameters. The thicknesses t_1 and t_2 are treated as interval parameters. The level of uncertainty is 2% variation about their nominal values due to the manufacturing tolerance specification. The nominal values of Young's modulus E, Poisson's ration υ and the yield stress σ_s are 207GPa, 0.30 and 487.7MPa, respectively. Due to the manufacturing and measurement errors, E, υ and σ_s are treated as bounded uncertain parameters using the ellipsoid model.

The uncertain level of their variations are described by

$$C = \left\{ \delta_E, \delta_\upsilon, \delta_{\sigma_2} : \{\delta_E, \delta_\upsilon, \delta_{\sigma_2}\} \begin{bmatrix} 1 & 0 & 0 \\ 0 & 1 & 0 \\ 0 & 0 & 1 \end{bmatrix} \begin{Bmatrix} \delta_E \\ \delta_\upsilon \\ \delta_{\sigma_2} \end{Bmatrix} \leq 0.1^2 \right\} \tag{22a}$$

and the NRMO problem is specified as follows:

$$\begin{aligned} &\min_{t_1,t_2} : \begin{cases} f_1(t_1,t_2,\sigma_s,E,\upsilon) = -E_d \\ f_2(t_1,t_2) = W \end{cases} \\ &\text{s.t. } \eta_1[g_m(t_1,t_2,\sigma_s,E,\upsilon) \leq 95kN] \geq \eta_{t1} \\ &0.5mm \leq t_1,t_2 \leq 2.5mm \end{aligned} \tag{22b}$$

The finite element simulation is carried out using the explicit non-linear finite element code LS-DYNA. This FE model is modeled using a number of Belytschko-Tsay four-node shell elements (5760). A $300kg$ lumped mass is attached to the

free end of the column during the crash analysis for the sake of supplying sufficient crushing energy. The deformation pattern is given in Fig. 10. In the process of optimization, the NSGA-II parameters are the same as those given in Table 1. Initially 40 sampling points are selected through LHD to construct the RSM surrogate models for the objectives and constraints within the given design domain and uncertainty space. The approximation model is a linear function of design variable $\mathbf{x}$, while surrogate models of E_d and g_m are nonlinear functions in terms of $\mathbf{t}$ and material parameters σ_s, E and υ. According to the RSM model, the larger the measurement values of R^2 and R^2_{adj}, the higher the modeling precision [Fang, Rais-Rohani, Liu, and Horstemeyer (2005)]. The regression analysis results are displayed in Table 4. It can be seen that the modeling precisions of the weight, maximum internal energy and average rigid wall force are all satisfied.

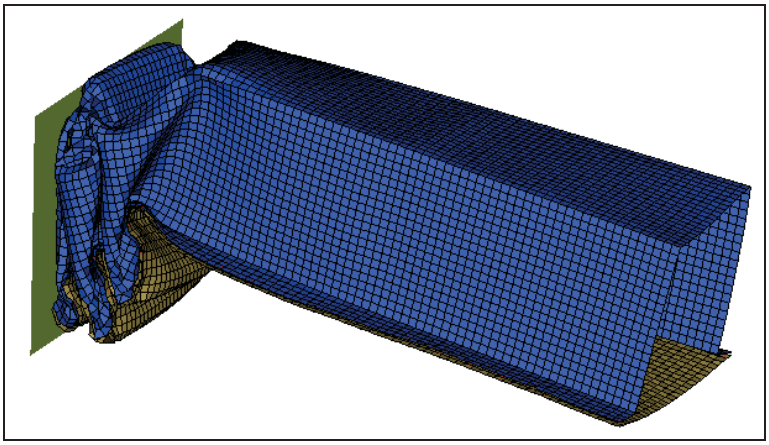

Figure 10: The finite element crushing model of the thin-walled column

The results under different reliability indices 1.0, 1.5 and 2.0 are summarized in Table 5. In Table 5, it shows that the energy absorption value is from -1.253×10^4J to -2.67×10^4J and the weight value is from $1.171kg$ to $3.748kg$ under $\eta_{t1}=1.0$. When $\eta_{t1}=1.5$, it can be found that the energy absorption value is from -1.253×10^4J to -2.54×10^4J and the weight W function value is from $1.171kg$ to $3.444kg$. When $\eta_{t1}=2.0$, the energy absorption value will be from -1.45×10^4J to -2.35×10^4J and the weight W is from $1.439kg$ to $3.041kg$. Fig. 11 plots the Pareto fronts with different reliability indices. Obviously, the ranges of the Pareto fronts also change with the different target reliability indices. Different reliability indices lead to different optimization results. When increasing the reliability index from 1.0 to 2.0, the minimum values of f_1 and f_2 increase from -2.67×10^4J to

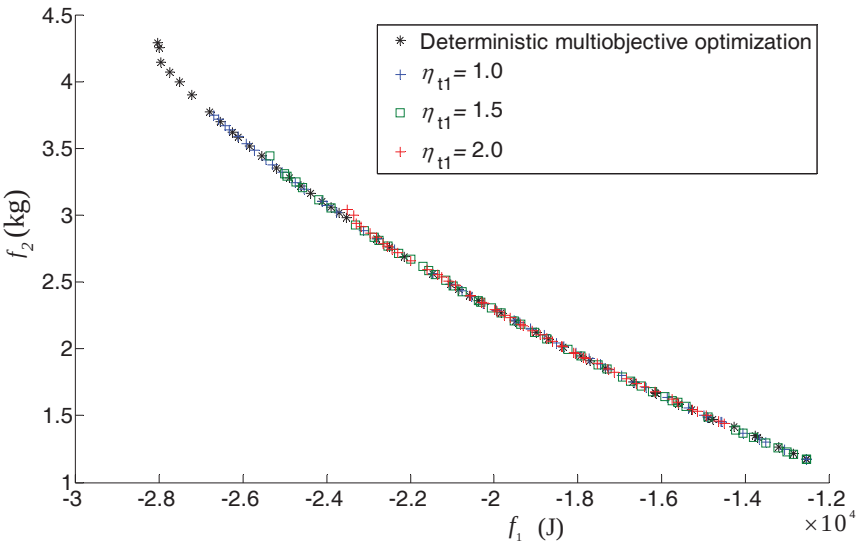

Figure 11: Pareto optimal front points for different reliability indices

$-2.35 \times 10^4 J$, and $1.17kg$ to $1.435kg$, respectively. This is because a larger reliability index produces a smaller feasible zone. If the target value of the reliability index is increased further, the optimal result will have a further change, which leads to more reasonable and reliable designs than the deterministic design optimization.

Table 4: Results of regression analysis

	R^2	R^2_{adj}	*Multiple R*
f_1	0.9875	0.9743	0.9937
f_2	1.0000	1.0000	1.0000
g_m	0.9793	0.9574	0.9896

4.4 Vehicle crashworthiness design application

In car crashing, it is expected that most of impact energy can be absorbed by the vehicle structure to reduce risk to occupants. Also the car is expected to be lightweight in its structure for energy efficiency. The energy absorption and lightweight actually conflict with each other and we have to find the Pareto solutions. The deceleration history was typically used as an indicator of impact severity, where the deceleration peak is required to be restricted to a certain level for crashworthiness

Table 5: Summary of results for the thin-walled column example

Pareto points	$\eta_{t1}=1.0$		$\eta_{t1}=1.5$	
x	(1.3412, 1.776)	(0.5, 0.5)	(1.0426, 1.7086)	(0.5, 0.5)
Min: $f_1(J)$	-2.67×10^4		-2.54×10^4	
Min: $f_2(kg)$		1.171		1.171
η_1	1.0009	1.8812	1.5003	1.8812
Pareto points	$\eta_{t1}=2.0$		*Deterministic*	
x	(0.8661, 1.5281)	(0.9060, 0.5)	(1.8320, 1.9127)	(0.5, 0.5)
Min: $f_1(J)$	-2.35×10^4		-2.805×10^4	
Min: $f_2(kg)$		1.4395		1.171
η_1	2.0003	2.9737	0	1.8812

design. Hence, the crashworthiness design is naturally characterized with multiple design requirements with structural uncertainty.

In this study, the maximum absorbing energy E_d by car parts and weight W of vehicle are chosen as two objectives, while the peak acceleration of B pillar is treated as constraint in this application. The vehicle front and end structures are important components for their roles on the energy absorption [Sun, Li, Hou, Zhou, Li, and Li (2010); Sun, Li, Stone, and Li (2010)]. As shown in Fig. 12, the thickness of three reinforced members around the frontal structure is chosen as the design variables (t_1,t_2,t_3) which could significantly affect the crash safety. The material properties and geometrical dimensions are assumed as uncertain-but-bounded parameters. The yield stress σ_{s1}, σ_{s2} and σ_{s3} are assumed to be bounded by an ellipsoid model as

$$\boldsymbol{\delta}_{\boldsymbol{\sigma}_s}=\{\delta_{\sigma_{s1}},\delta_{\sigma_{s2}},\delta_{\sigma_{s3}}\}\in C=\{\boldsymbol{\delta}_{\boldsymbol{\sigma}_s}:\boldsymbol{\delta}_{\boldsymbol{\sigma}_s}^T\mathbf{W}_{\boldsymbol{\delta}_s}\boldsymbol{\delta}_{\boldsymbol{\sigma}_s}\le 0.1^2\} \tag{23a}$$

where the nominal values are $\bar{\sigma}_{s1}=343MPa$, $\bar{\sigma}_{s2}=286MPa$ and $\bar{\sigma}_{s3}=462MPa$, and the characteristic matrix is $\mathbf{W}_{\boldsymbol{\delta}_s}=[1\,0\,0;1\,0\,0;1\,0\,0]$. Due to manufacturing tolerance specifications, the thicknesses of the three reinforced members are regarded as interval parameters with 3% variation about their nominal values. Therefore, there are a total number of 6 uncertain parameters to be modeled using the ellipsoid and interval methods, respectively.

As a result, the optimization problem can be formulated by

$$\begin{aligned} \min_{t_1,t_2,t_3} \; & :f_1(t_1,t_2,t_3,\sigma_{s1},\sigma_{s2},\sigma_{s3}) = -E_d \\ & f_2(t_1,t_2,t_3) = W \\ \text{s.t. } & \eta_1[g_a(t_1,t_2,t_3,\sigma_{s1},\sigma_{s2},\sigma_{s3}) \le 40g] \ge \eta_{t1} \\ & 0.5mm \le t_1,t_2,t_3 \le 3.0mm \end{aligned} \tag{23b}$$

The FEM simulation is carried out using the software LS-DYNA. The FEA model of a Dodge Grand Caravan was developed by NCAC (National Crash Analysis Center). The FE model of the vehicle was obtained from: www.ncac.gwu.edu/archives/model/index.html. It has 344724 nodes and 339969 (mostly shell) elements. The initial velocity is $56.66km/h$. This model is used for full-frontal impact (FFI) simulations and the results were found to be consistent with physical crash test data by NCAC. In this study, we used the FEA model (Fig. 13) in simulations of FFI. The deformation of the full frontal impact is given in Fig. 14. A simulation of 120ms FFI takes approximately 3 hours with 4 processors Intel Core^{TM}i7-2600 3.40 GHz.

Here, 50 sampling points of crash simulations are obtain via LHD, thus the approximation models are created with the material parameters $\boldsymbol{\sigma}_\mathbf{s}$ and current design variables $\mathbf{t}$. The approximation model of mass is a linear function of design variables $\mathbf{t}$. The approximation models for the maximum internal energy and acceleration are nonlinear function with respect to $\mathbf{t}$ and $\boldsymbol{\sigma}_\mathbf{s}$. Hence, the NSGA-II will be used to generate the design variable $\mathbf{x}$ in the outer layer, and the evaluations of the non-probabilistic reliability index will be treated in the inner layer. Thus the Pareto optimal points of the weight and the maximum internal energy can be achieved under the reliability constraints. For the NSGA-II specific parameters, the reader can refer to Table 1.

Although the Pareto set can provide designers with a number of inferior design solutions to assist the decision-make in the initial stage of the design circle, the decision must be made with respect to the most satisfactory solution (termed as "knee point") from Pareto-set finally [Sun, Li, Hou, Zhou, Li, and Li (2010); Sun, Li, Stone, and Li (2010)]. The deterministic knee point and reliability knee point are obtained from the Pareto sets, respectively. The results are summarized in Table 6 to compare with the baseline model. The optimal results obtained by the proposed reliability-based optimization with the reliability index $\eta_{t1} = 1.0$ (Fig. 15), as well as the deterministic design are given in Table 6. Without considering uncertainties, the reliability indices corresponding to the initial and the deterministic designs are negative and 0.1629, respectively. This means both designs fail to satisfy the reliability requirements and thus are unreliable. In other word, both the initial and the deterministic optimal designs show a certain violation of the reliability constraints.

In the design obtained by the present method, the reliability index is 1.0821. The results listed in Table 6 shows that the NRMO method can produce a more reliable design than the deterministic approach. Again, the results of this case show the effectiveness of the proposed method.

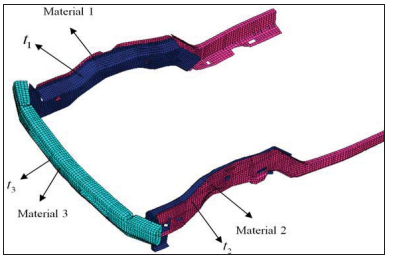

Figure 12: Design variables and material

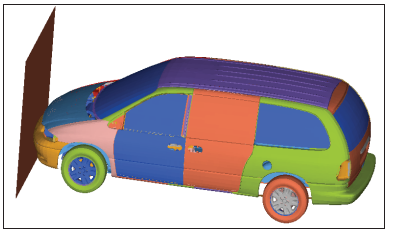
Figure 13: Finite element model of vehicle

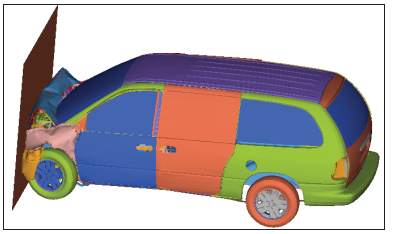
Figure 14: The deformation of the full frontal impact

5 Conclusions

This paper proposes a new design optimization method for NRMO problems in the presence of uncertainty, which can be regarded as a useful supplement to the

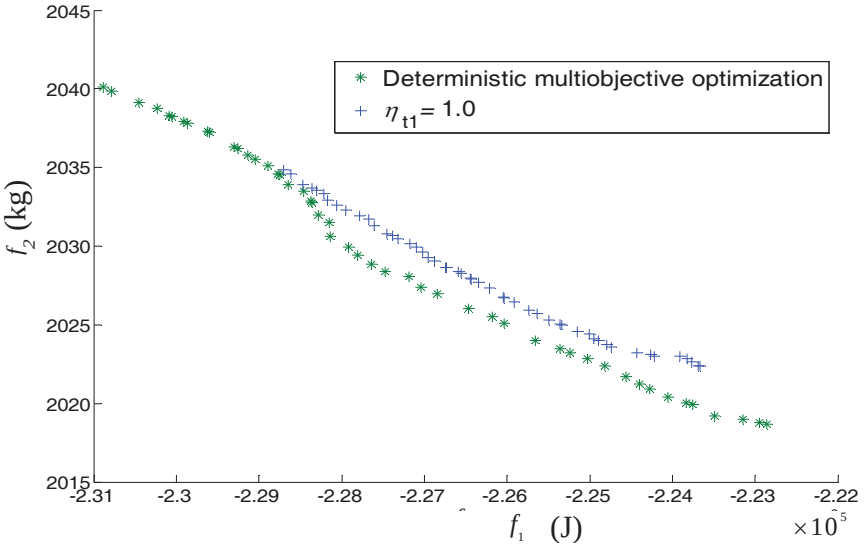

Figure 15: Comparison of Pareto fronts of deterministic, and reliability optimizations when $\eta_{t1} = 1.0$

Table 6: Optimization for the crashworthiness of vehicle

Design parameter	*Optimal component thickness (mm)*		
	Initial design	*Non-deterministic*	*Deterministic*
t_1	2.0	2.9963	2.9808
t_2	2.0	1.5371	1.0039
t_3	2.0	1.7544	2.2751
$-E_d(J)$	-2.2019×10^5	-2.2634×10^5	-2.2684×10^5
$W(kg)$	2012.2	2027.71	2026.96
Reliability index η_1	-0.1439	1.0821	0.1629

RBO approaches. The convex models are applied to count the uncertainties of uncertain-but-bounded parameters, in which only bounds of parameters are needed, without necessarily knowing their precise probability distributions. Based on non-probabilistic reliability index method, the NRMO problem is transformed into an equivalent deterministic optimization problem. Thus efficient NRMO algorithm is formulated as a nested double-loop optimization problem. The NSGA-II algorithm is applied to the outer loop to evaluate the approximations of the objective functions and constraints, based on the RSM surrogate model. The SQP is applied to the inner loop to evaluate the non-probabilistic reliability index. Then the Pareto set can be obtained with the prescribed reliability index.

Several numerical examples have been applied to demonstrate the feasibility and the validity of the proposed method. From Pareto sets with different target reliabilities, it can be found that the "reliable" Pareto optimal front with different target reliabilities leads to a combination of “translational” and “rotational” shifts. When taking uncertainty into account, the "optimal" Pareto font will shift towards a "safer" region where parameter uncertainties no longer impact the feasibility of the optimal solutions. The engineering application in crashworthiness design also shows the ability of the present method to some engineering design problems.

Acknowledgement: This work is partially supported by The National Natural Science Foundation of China(11302033),Hunan Provincial Natural Science Foundation of China (12JJ3044), The Open Fund in the Key Laboratory of Manufacture and Test Techniques for Automobile Parts (Chongqing University of Technology), Ministry of Education(2010KLMT13), The Open Fund of State Key Laboratory of Automotive Simulation and Control(20121105), The Open Fund of Engineering Research Center of Catastrophic Prophylaxis and Treatment of Road & Traffic Safety (Changsha University of Science & Technology) (kfj110303), Ministry of Education, and The Open Fund of the Key Laboratory for Safety Control of Bridge Engineering (Changsha University of Science & Technology), Ministry of Education and Hunan Province (12KB04).

References

Au, F. T. K.; Cheng, Y. S.; Tham, L. G.; Zeng, G. W. (2003): Robust design of structures using convex models. *Computers and Structures*, vol. 81, no. 28-29, pp. 2611–2619.

Barakat, S.; Bani-Hani, K.; Taha, M. Q. (2004): Multi-objective reliability-based optimization of prestressed concrete beams. *Structural Safety*, vol. 26, no. 3, pp. 311–342.

Ben-Haim, Y. (1994): A non-probabilistic concept of reliability. *Structural Safety*, vol. 14, no. 4, pp. 227–245.

Ben-Haim, Y.; Elishakoff, I. (1990): *Convex models of uncertainties in applied mechanics*. Elsevier Science Publisher, Amsterdam.

Boggs, P. T.; Tolle, J. W. (1995): Sequential quadratic programming. *Acta Numerica*, vol. 4, pp. 1–51.

Chau, M. Q.; Han, X.; Bai, Y. C.; Jiang, C. (2012): A structural reliability analysis method based on radial basis function. *CMC: Computers, Materials & Continua*, vol. 27, no. 2, pp. 128–142.

Chen, W.; Sahai, A.; Messac, A.; Sundararaj, G. (2000): Exploration of the effectiveness of physical programming in robust design. *Journal of Mechanical Design*, vol. 122, pp. 155–164.

Deb, K. (2001): *Multi-objective optimization using evolutionary algorithms*. Wiley, New York.

Deb, K.; Padmanabhan, D.; Gupta, S.; Mall, A. (2007): Reliability-based multi-objective optimization using evolutionary algorithms. *Evolutionary Multi-Criterion Optimization Proceedings*, vol. 4403, pp. 66–80.

Deb, K.; Pratap, A.; Agarwal, S.; Meyarivan, T. (2002): A fast and elitist multiobjective genetic algorithm: Nsga-ii. *Evolutionary Computation, IEEE Transactions on*, vol. 6, no. 2, pp. 182–197.

Draper, N. R.; Smith, H. (1998): *Applied regression analysis*. Wiley, New York.

Du, X.; Sudjianto, A.; Huang, B. (2005): Reliability-based design with the mixture of random and interval variables. *Journal of Mechanical Design*, vol. 127, no. 6, pp. 1068–1076.

Elishakoff, I. (1995): Discussion on: a non-probabilistic concept of reliability. *Structural Safety*, vol. 17, no. 2, pp. 195–199.

Elishakoff, I.; Haftka, R. T.; Fang, J. (1994): Structural design under bounded uncertainty-optimization with anti-optimization. *Computers and Structures*, vol. 53, no. 6, pp. 1401–1405.

Fang, H.; Rais-Rohani, M.; Liu, Z.; Horstemeyer, M. F. (2005): A comparative study of metamodeling methods for multiobjective crashworthiness optimization. *Computers and Structures*, vol. 83, no. 25-26, pp. 2121–2136.

Fang, J.; Gao, Y.; Sun, G.; Li, Q. (2013): Multiobjective reliability-based optimization for design of a vehicledoor. *Finite Elements in Analysis and Design*, vol. 67, no. 0, pp. 13–21.

Gao, W. (2007): Natural frequency and mode shape analysis of structures with uncertainty. *Mechanical Systems and Signal Processing*, vol. 21, no. 1, pp. 24–39.

Gao, W.; Song, C.; Tin-Loi, F. (2010): Probabilistic interval analysis for structures with uncertainty. *Structural Safety*, vol. 32, no. 3, pp. 191–199.

Gao, W.; Song, C. M.; F. Tin-Loi, F. (2009): Probabilistic interval response and reliability analysis of structures with a mixture of random and interval properties. *CMES-Computer Modeling in Engineering & Sciences*, vol. 46, no. 2, pp. 151–189.

Jiang, C.; Han, X.; Liu, G. R. (2007): Optimization of structures with uncertain constraints based on convex model and satisfaction degree of interval. *Computer*

Methods in Applied Mechanics and Engineering, vol. 196, no. 49-52, pp. 4791–4800.

Jiang, C.; Han, X.; Liu, G. R.; Liu, G. P. (2008): A nonlinear interval number programming method for uncertain optimization problems. *European Journal of Operational Research*, vol. 188, no. 1, pp. 1–13.

Kang, Z.; Luo, Y. (2009): Non-probabilistic reliability-based topology optimization of geometrically nonlinear structures using convex models. *Computer Methods in Applied Mechanics and Engineering*, vol. 198, no. 41-44, pp. 3228–3238.

Kang, Z.; Luo, Y.; Li, A. (2011): On non-probabilistic reliability-based design optimization of structures with uncertain-but-bounded parameters. *Structural Safety*, vol. 33, no. 3, pp. 196–205.

Khakhal, A.; Nariman-zadeh, N.; Darvizeh, A.; Masoumi, A.; Notghi, B. (2010): Reliability-based robust multi-objective crashworthiness optimisation of s-shaped box beams with parametric uncertainties. *International Journal of Crashworthiness*, vol. 15, no. 4, pp. 443–456.

Lagaros, N. D.; Garavelas, A. T.; Papadrakakis, M. (2008): Innovative seismic design optimization with reliability constraints. *Computer Methods in Applied Mechanics and Engineering*, vol. 198, no. 1, pp. 28–41.

Li, F.; Luo, Z.; Rong, J.; Zhang, N. (2013): Interval multi-objective optimisation of structures using adaptive kriging approximations. *Computers and Structures*, vol. 119, pp. 68–84.

Li, F.; Luo, Z.; Sun, G. (2011): Reliability-based multiobjective design optimization under interval uncertainty. *CMES-Computer Modeling in Engineering and Science*, vol. 74, no. 1, pp. 39–64.

Li, M.; Azarm, A. (2008): Multiobjective collaborative robust optimization with interval uncertainty and interdisciplinary uncertainty propagation. *Journal of Mechanical Design*, vol. 130, pp. 719–729.

Liao, X.; Li, Q.; Yang, X.; Zhang, W.; Li, W. (2008): Multiobjective optimization for crash safety design of vehicles using stepwise regression model. *Structural and Multidisciplinary Optimization*, vol. 35, no. 6, pp. 561–569.

Lin, J.; Luo, Z.; Tong, L. (2010): A new multi-objective programming scheme for topology optimization of compliant mechanisms. *Structural and Multidisciplinary Optimization*, vol. 40, no. 1, pp. 241–255.

Lombardi, M. (1998): Optimization of uncertain structures using non-probabilistic models. *Computers and Structures*, vol. 67, no. 1-3, pp. 99–103.

Luo, Y.; Kang, Z.; Luo, Z.; Li, A. (2009): Continuum topology optimization with non-probabilistic reliability constraints based on multi-ellipsoid convex model. *Structural and Multidisciplinary Optimization*, vol. 39, no. 3, pp. 297–310.

Luo, Z.; Chen, L.; Yang, J.; Zhang, Y.; Abdel-Malek, K. (2005): Compliant mechanism design using multi-objective topology optimization scheme of continuum structures. *Structural and Multidisciplinary Optimization*, vol. 30, no. 2, pp. 142–154.

Marler, R. T.; Arora, J. S. (2004): Survey of multi-objective optimization methods for engineering. *Structural and Multidisciplinary Optimization*, vol. 26, no. 6, pp. 369–395.

Möller, B.; Beer, M. (2008): Engineering computation under uncertainty – capabilities of non-traditional models. *Computers and Structures*, vol. 86, no. 10, pp. 1024–1041.

Morris, M. D.; Mitchell, T. J. (1995): Exploratory designs for computational experiments. *Journal of Statistical Planning and Inference*, vol. 43, no. 3, pp. 381–402.

Myers, R. H.; Montgomery, D. C. (1995): *Response surface methodology: process and product optimization using designed experiments*. Wiley, New York.

Olyaie, M. S.; Razfar, M. R.; Kansa, E. J. (2011): Reliability based topology optimization of a linear piezoelectric micromotor using the cell-based smoothed finite element method. *CMES: Computer Modeling in Engineering & Sciences*, vol. 75, no. 1, pp. 43–88.

Qiu, Z.; Yang, D.; Elishakoff, I. (2008): Probabilistic interval reliability of structural systems. *International Journal of Solids and Structures*, vol. 45, no. 10, pp. 2850–2860.

Santos, S. R.; Matioli, L. C.; Beck, A. T. (2012): New optimization algorithms for structural reliability analysis. *CMES: Computer Modeling in Engineering & Sciences*, vol. 83, no. 1, pp. 23–55.

Schuëller, G. I.; Jensen, H. A. (2008): Computational methods in optimization considering uncertainties – an overview. *Computer Methods in Applied Mechanics and Engineering*, vol. 198, no. 1, pp. 2–13.

Simpson, T. W.; Poplinski, J. D.; Koch, P. N.; Allen, J. K. (2001): Metamodels for computer-based engineering design: Survey and recommendations. *Engineering with Computers*, vol. 17, no. 2, pp. 129–150.

Sinha, K. (2007): Reliability-based multiobjective optimization for automotive crashworthiness and occupant safety. *Structural and Multidisciplinary Optimization*, vol. 33, no. 3, pp. 255–268.

Sun, G.; Li, G.; Hou, S.; Zhou, S.; Li, W.; Li, Q. (2010): Crashworthiness design for functionally graded foam-filled thin-walled structures. *Materials Science and Engineering: A*, vol. 527, no. 7-8, pp. 1911–1919.

Sun, G.; Li, G.; Stone, M.; Li, Q. (2010): A two-stage multi-fidelity optimization procedure for honeycomb-type cellular materials. *Computational Materials Science*, vol. 49, no. 3, pp. 500–511.

Taboada, H. A.; Baheranwala, F.; Coit, D. W.; Wattanapongsakorn, N. (2007): Practical solutions for multi-objective optimization: An application to system reliability design problems. *Reliability Engineering and System Safety*, vol. 92, no. 3, pp. 314–322.

Valdebenito, M.; Schuëller, G. (2010): A survey on approaches for reliability-based optimization. *Structural and Multidisciplinary Optimization*, vol. 42, no. 5, pp. 645–663.

Wang, C.; Gao, W.; Yang, C.; Song, C. (2011): Non-deterministic structural response and reliability analysis using a hybrid perturbation-based stochastic finite element and quasi-monte carlo method. *Computers Materials and Continua*, vol. 25, no. 1, pp. 19.

Wu, J.; Luo, Z.; Zhang, Y.; Zhang, N.; Chen, L. (2013): Interval uncertain method for multibody mechanical systems using chebyshev inclusion functions. *International Journal for Numerical Methods in Engineering*, vol. 95, no. 7, pp. 608–630.

Wu, J.; Zhang, Y.; Chen, L.; Luo, Z. (2013): A chebyshev interval method for nonlinear dynamic systems under uncertainty. *Applied Mathematical Modelling*, vol. 37, no. 6, pp. 4578–4591.

Xiang, Y.; Wang, Q.; Fan, Z.; Fang, H. (2006): Optimal crashworthiness design of a spot-welded thin-walled hat section. *Finite Elements in Analysis and Design*, vol. 42, no. 10, pp. 846–855.